

UC Berkeley

Working Papers

Title

Lateral Control Of Commuter Buses

Permalink

<https://escholarship.org/uc/item/8v96f9md>

Authors

Hingwe, Pushkar
Tomizuka, Masayoshi

Publication Date

1995

CALIFORNIA PATH PROGRAM
INSTITUTE OF TRANSPORTATION STUDIES
UNIVERSITY OF CALIFORNIA, BERKELEY

Lateral Control of Commuter Buses

**Pushkar Hingwe,
Masayoshi Tomizuka**

**California PATH Working Paper
UCB-ITS-PWP-95-9**

This work was performed as part of the California PATH Program of the University of California, in cooperation with the State of California Business, Transportation, and Housing Agency, Department of Transportation; and the United States Department Transportation, Federal Highway Administration.

The contents of this report reflect the views of the authors who are responsible for the facts and the accuracy of the data presented herein. The contents do not necessarily reflect the official views or policies of the State of California. This report does not constitute a standard, specification, or regulation.

Report for MOU 129

July 1995

ISSN 1055-1417

**This paper uses Postscript Type 3 fonts.
Although reading it on the screen is difficult
it will print out just fine.**

Lateral Control of Commuter Buses

Pushkar Hingwe
Masayoshi Tomizuka

California Partners for Advanced Transit and Highways (PATH)
Mechanical Engineering Department
University of California at Berkeley

Lateral Control of Commuter Buses

Pushkar Hingwe
Masayoshi Tomizuka

California Partners for Advanced Transit and Highways (PATH)
Mechanical Engineering Department
University of California at Berkeley March 1995

Abstract

This report presents two approaches to the design of the lateral controllers for commuter buses based on Sliding Mode Control (SMC). The objective of the control is to track the lane centerline. SMC is selected because of passenger load uncertainties and variations in the road tire interaction. Importance is given to reduction or elimination of the control chatter inherent in the SMC systems involving switching functions. The first controller uses the sensor output which is a combination of yaw and lateral error. The combined error is forced to stay on a manifold by SMC. The second controller achieves tracking objective by providing a yaw rate to the vehicle so as to keep the lateral error dynamics stable. The two controllers are shown to differ only in the position of an integrator which gets naturally introduced in the closed loop. The controllers are compared by performing simulations for a range of parameters. It is concluded that though the performance of the controllers is comparable for the present application, one of them is theoretically better.

Keywords: Advanced Vehicle Control Systems, Sliding Mode Control, Chatter reduction. Lateral control.

Executive Summary

Lateral control of vehicles in the light of Intelligent Transportation Systems (ITS) and Automated Highway Systems (AHS) has been an active research subject in recent years. Much of the work in past has been concentrated in the area of light vehicles. Peng and Tomizuka (1993) applied Frequency Shaped Linear Quadratic (FSLQ) control to the problem of lateral (steering) control of the passenger car. Pham et al. (1994) applied Sliding Mode Control (SMC) to the problem of combined lateral and longitudinal control of passenger cars. Ackermann et al. (1995) applied SMC in a different manner from to the problem of the lateral control of passenger cars. In this report lateral control of the commuter buses is considered. The motivation for a separate consideration to the problem of lateral control of buses comes through the following. Commuter buses are roughly 10 times heavier than the passenger vehicles. Hence the system response to the steering angle command is sluggish. Also there is greater likelihood of tire force saturation during cornering. The behavior of the vehicle is nonlinear at the saturation point of the tires. Furthermore, bus parameters such as the mass and moments of inertia change often and over wider ranges (mass could change from 10,000 kg. to 16,000 kg.) and the buses are more prone to roll over than passenger vehicles. Due to the above mentioned characteristics, robust or adaptive control is essential for the lateral control of commuter buses. In this report, we study the use of the SMC methodology, which is known for its robustness to parametric uncertainties. Two SMC based approaches are considered and compared to each other. Only lateral and yaw dynamics of the buses are considered in the design of these controllers. One design is similar to what was used by (Pham et al. 1994) for control of passenger vehicles. A linear combination of lateral error and yaw error which in effect gives the lateral displacement of a point other than the center of gravity (CG) of the vehicle is fed back to the controller which sets the command for the steering angle. The combined error becomes input to the SMC. In the second SMC approach, the steering angle rate becomes the control command as against the steering angle in the first approach. We apply this control algorithm to the problem of the lateral control of commuter buses. In this controller, the problem is reformatted into a strict feedback form so that the desired yaw rate can be set to make the lateral dynamics stable. The SMC is set so that the actual yaw rate matches the desired rate.

A feature common between the two SMC approaches is that an integrator can be naturally introduced in the feedback loop. The integrator is ideally suited to counteract disturbances such as wind gusts. While SMC is effective for such disturbances, the presence of integral control assures static robust performance when the signum function, which appears in SMC, is replaced by saturation function to eliminate chattering. The introduction of the integrator in the second SMC design is somewhat more natural. Apart from retaining the asymptotic tracking property while filtering the chatter, it can be thought of as actuator dynamics and would thus give a better representation of the actual system in the simulations. Simulation results confirm that the two SMC based controllers provide excellent lane following performance.

1 Introduction

Lateral control of vehicles in the light of Intelligent Transportation Systems (ITS) and Automated Highway Systems (AHS) has been an active research subject in recent years (Peng and Tomizuka, 1993). Much of the work in past has been concentrated in the area of light vehicles. Peng and Tomizuka (1993) applied Frequency Shaped Linear Quadratic (FSLQ) control to the problem of lateral (steering) control of passenger cars. Pham et al. (1994) applied Sliding Mode Control (SMC) to the problem of combined lateral and longitudinal control of passenger cars. Ackermann et al. (1995) applied SMC in a different manner from Pham et al. (1994) to the problem of the lateral control of passenger cars. In this report lateral control of commuter buses is considered. Commuter buses are roughly 10 times heavier than the passenger vehicles. Hence the system response to the steering angle command is sluggish. Also there is more likelihood of tire force saturation during cornering. The behavior of the vehicle is nonlinear at the saturation point of the tires (Peng, 1992), (Bareket and Fancher, 1989). Furthermore, bus parameters such as the mass and moments of inertia change often and over wider ranges and the buses are more prone to roll over than passenger vehicles. Due to the above mentioned characteristics, robust or adaptive control is essential for the lateral control of commuter buses. In this report, we study the use of the SMC methodology, which is known for its robustness to parametric uncertainties. Two SMC based approaches are considered and compared to each other. Only the lateral and yaw dynamics of the buses are considered in the design of these controllers. One design is similar to what was used by Pham et al. (1994) for control of passenger vehicles. A linear combination of lateral error and yaw error which in effect gives the lateral displacement of a point other than the center of gravity (CG) of the vehicle is fed back to the controller. The combined error becomes input to the SMC. Another control presented is in the line of Ackermann et al. (1995). We apply this control algorithm to the problem of the lateral control of commuter buses. In this controller, the problem is reformatted into a strict feedback form so that the desired yaw rate can be set to make the lateral dynamics stable. The SMC is set so that the actual yaw rate matches the desired.

A feature common between the two SMC approaches is that an integrator can be naturally introduced in the feedback loop. The integrator is ideally suited to counteract disturbances such as wind gusts. While SMC is effective for such disturbances, the presence of integral control assures static robust performance when the signum function, which appears in SMC, is replaced by saturation function to eliminate chattering.

The remainder of the report is organized as follows. Section 2 states the problem formulation along with the dynamic model of a commuter bus. The SMCs are developed in section 3. Section 4 presents simulation of the closed loop system for a commuter bus model (Daimler Benz) under various conditions of speed and mass. Conclusions are presented in section 5.

2 Lateral Control Problem for Commuter Buses

In general the control objectives in lateral control of road vehicles for lane following are as follows:

1. Keeping lateral error at a selected point, e.g. at the center of gravity (CG) close to zero.
2. Maintaining the vehicle orientation parallel to the road orientation.
3. Ensuring passenger comfort.

It is known that the orientation error, i.e. the yaw of the vehicle relative to the road orientation, cannot be made zero on a curve (at steady state) for vehicles which have front wheel steering only (Matsumoto and Tomizuka, 1992). Thus the goal is to keep the lateral error of a certain point on the vehicle body zero while maintaining as narrow a bound as possible on the yaw error.

2.1 The vehicle model

In this section, we describe the dynamic equations and the parameters of the vehicle model.

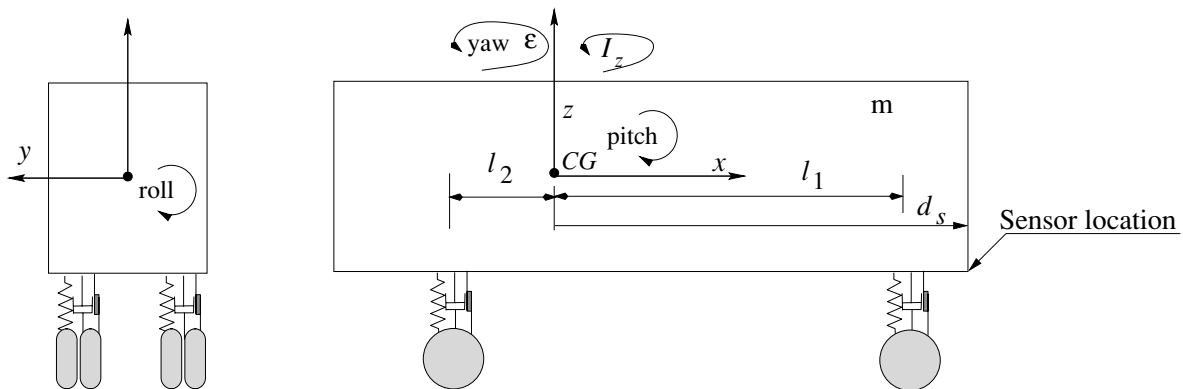


Figure 1: The bus model and description of parameters

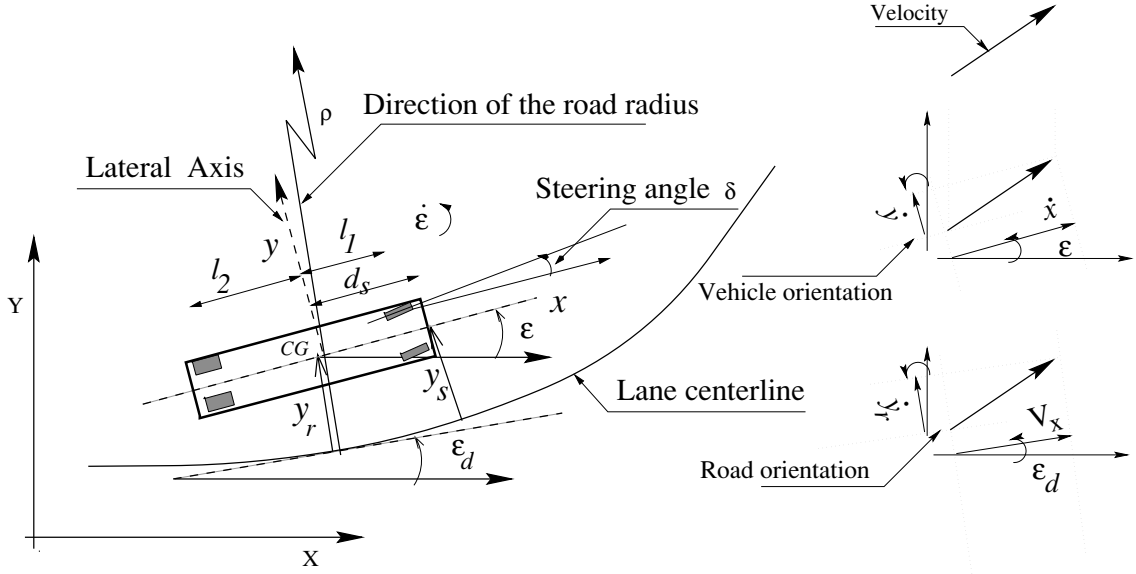


Figure 2: The description of the states, input and the output

The complex and simplified models of the passenger vehicle were derived by Peng (1992) and Patwardhan (1994). The vehicle model for the commuter bus is essentially the same with modification to accommodate weight shift due to roll and substitution of the tire model in (Peng, 1992) by a tire model suited to buses. Details of the tire model appropriate for commuter buses are given in (Bareket and Fancher, 1989). The model given in figure 1 shows all the translational and rotational modes of the bus and it has twelve states, two for each rotational and translational degree of freedom. We will use this complex model in simulations. Open loop simulations show that the pitch dynamics are negligible. Roll dynamics though not as small are not considered because the coupling between the roll and the steering input is rather weak. Thus, for the controller design, we consider only the lateral and yaw dynamics. The dynamic equations of the bus model for control design purpose are:

$$\begin{aligned}
 m\ddot{y} &= -m\dot{\epsilon}V_x - K_{wy}\dot{y}|\dot{y}| - 2C_{\alpha_r}(\dot{y} - \dot{\epsilon}l_2)/V_x - 2C_{\alpha_f}(\dot{y} + \dot{\epsilon}l_1)/V_x + 2C_{\alpha_f}\delta \\
 \ddot{y} &\triangleq f_1(\mathbf{x}) + b_1\delta \\
 I_z\ddot{\epsilon} &= 2l_2C_{\alpha_r}(\dot{y} - \dot{\epsilon}l_2)/V_x - 2l_1C_{\alpha_f}(\dot{y} + \dot{\epsilon}l_1)/V_x + 2l_1C_{\alpha_f}\delta \\
 \ddot{\epsilon} &\triangleq f_2(\mathbf{x}) + b_2\delta
 \end{aligned} \tag{1}$$

where,

\dot{y} = Vehicle velocity along the lateral principle axis of the sprung mass of the vehicle in m/s ,

\ddot{y} = Vehicle linear acceleration in the lateral principle direction m/s^2 ,

$\dot{\epsilon}$ = Yaw rate of the vehicle in rad/s (refer figure 2),

$\ddot{\epsilon}$ = Angular acceleration of the vehicle in the yaw direction in rad/s^2 ,

V_x = Longitudinal velocity of the vehicle (component along the road) in m/s ,

m = Mass of the vehicle kg (10,000 – 16,000),

I_z = Yaw moment of inertia in kgm^2 (171,050),

l_1 = Longitudinal distance of the front axle from the center of gravity in m (3.67),

l_2 = Longitudinal distance of the rear axle from the center of gravity in m (1.93),

C_{α_r} = Cornering stiffness of the rear tires in KN/rad (425),

C_{α_f} = Cornering stiffness of the front tires in KN/rad (213),
 K_{wy} = Wind drag coefficient in Ns^2/m^2 ,
 δ = steering angle (input) rad ,
 $f_1(\mathbf{x}) \triangleq (-m\dot{\epsilon}V_x - K_{wy}\dot{y}|\dot{y}| - 2C_{\alpha_r}(\dot{y} - \dot{\epsilon}l_2)/V_x - 2C_{\alpha_f}(\dot{y} + \dot{\epsilon}l_1)/V_x) / m$,
 \mathbf{x} is the state vector comprising of $[y, \dot{y}, \epsilon, \dot{\epsilon}]$,
 $b_1 \triangleq 2C_{\alpha_f}/m$,
 $f_2(\mathbf{x}) \triangleq (2l_2C_{\alpha_r}(\dot{y} - \dot{\epsilon}l_2)/V_x - 2l_1C_{\alpha_f}(\dot{y} + \dot{\epsilon}l_1)/V_x) / I_z$ and
 $b_2 \triangleq (2l_1C_{\alpha_f})/I_z$.

The values in the parentheses are nominal or the range of values. Since we will be interested in keeping the lateral error of a certain point on the vehicle zero, we define the lateral error at this point as y_s . This point is located d_s distance ahead of the CG of the vehicle and is shown in figure 1. A lateral error sensor is located at this point. Note that y_s is defined as

$$y_s = y_r + d_s(\epsilon - \epsilon_d) \quad (2)$$

where,

y_r = Lateral position of the center of gravity of the vehicle with respect to the road center.
 d_s is the distance of the lateral error sensor from the CG of the vehicle (as shown in figure 1).
 ϵ_d is the yaw angle of the road with respect to a global coordinate system (see figure 2).
 ϵ is the yaw angle of the vehicle with respect to the same global coordinate system as in the definition of ϵ_d .

The road orientation ϵ_d is never going to be present in our formulation except when occurring as $\pm(\epsilon - \epsilon_d)$. But we will be needing its time derivatives. Road yaw rate, given by $\dot{\epsilon}_d = V_x \rho$ where ρ is the road curvature, is assumed available. For the control design, we will require that the third time derivative of the the desired yaw be piecewise continuous. In practice, the road curvature data can be filtered to achieve the desired smoothness. One method to filter the road curvature which changes discontinuously is to have preview information for a fixed distance ahead and then use this to smooth out the radius of curvature. This is (approximately) illustrated in figure 3. This is not unreasonable as in the present ITS scenario, (particularly so in the context of Partners for Advanced Transit and Highways (PATH) of California), the availability of road curvature data ahead of time is assumed.

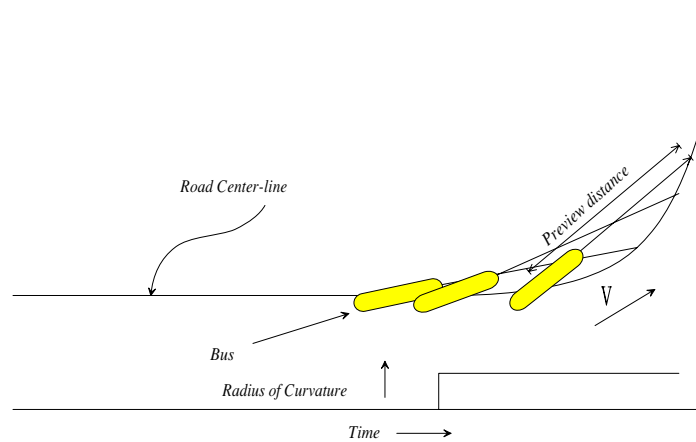


Figure 3: Filtering the road curvature “disturbance” by “preview”

3 Controller Design

We present two SMC based controllers in this section for lateral control of buses. As stated earlier, one of the aims of the controller is to keep the bus lateral error zero and yaw error bounded at all times. Ride comfort has to be maintained. Additionally steering angle is limited to approximately 0.5 rad and the steering angle rate to 0.5 rad/s .

The assumptions for the controller design are :

- All states are assumed available.
- $f_2(\mathbf{x})$ is sufficiently smooth.
- Road yaw rate, $\dot{\epsilon}_d$, which will occur in the controller design is sufficiently smooth.

3.1 Sliding Mode Controller Design - I

The formulation of the control law follows from Pham et al. (1994). One goal is to make the combined lateral and longitudinal error zero. In order to use notation consistent with Slotine (Slotine and Li, 1991), obtain the dynamic equation for y_s .

Noting the definition of y_s given in equation (2),

$$\dot{y}_s = \dot{y}_r + d_s(\dot{\epsilon} - \dot{\epsilon}_d). \quad (3)$$

From geometry, (refer figure 2),

$$\begin{aligned} \dot{y}_r &= \dot{y} \cos(\epsilon - \epsilon_d) + \dot{x} \sin(\epsilon - \epsilon_d) \\ V_x &= -\dot{y} \sin((\epsilon - \epsilon_d)) + \dot{x} \cos((\epsilon - \epsilon_d)) \end{aligned} \quad (4)$$

From equations(3) and (4) we get,

$$\ddot{y}_s = \ddot{y} \cos(\epsilon - \epsilon_d) + \ddot{x} \sin(\epsilon - \epsilon_d) + (\dot{\epsilon} - \dot{\epsilon}_d)(-\dot{y} \sin(\epsilon - \epsilon_d) + \dot{x} \cos(\epsilon - \epsilon_d)) + d_s(\ddot{\epsilon} - \ddot{\epsilon}_d)$$

Assuming \ddot{x} and $(\epsilon - \epsilon_d)$ are small, we get,

$$\begin{aligned} \ddot{y}_s &\approx \ddot{y} + (\dot{\epsilon} - \dot{\epsilon}_d)V_x + d_s(\ddot{\epsilon} - \ddot{\epsilon}_d) \\ &= f_1(\mathbf{x}) + b_1\delta + d_s(f_2(\mathbf{x}) + b_2\delta - \ddot{\epsilon}_d) + V_x(\dot{\epsilon} - \dot{\epsilon}_d). \end{aligned} \quad (5)$$

We define

$$\begin{aligned} b &= b_1 + d_s b_2 \\ f(\mathbf{x}) &= f_1(\mathbf{x}) + d_s f_2(\mathbf{x}) + V_x(\dot{\epsilon} - \dot{\epsilon}_d) - d_s \ddot{\epsilon}_d \end{aligned} \quad (6)$$

Thus we can write the plant equations as

$$\begin{aligned}\frac{d}{dt}y_s &= \dot{y}_s \\ \frac{d}{dt}\dot{y}_s &= f(\mathbf{x}) + b\delta\end{aligned}\tag{7}$$

Note that due to uncertainties in the bus parameters, we know only the estimates of $f(\mathbf{x})$ and b in terms of the nominal values of the plant parameters and current state. Let these be $\hat{f}(\mathbf{x})$ and \hat{b} . We see that the plant as described above has relative degree two with respect to the given input output pair δ and y_s .

Define sliding surface variable s as

$$s \triangleq \dot{e} + \lambda e, \quad \lambda > 0.\tag{8}$$

Where e , the tracking error, is the difference in the actual lateral error at the sensor y_s and the desired lateral error at the sensor y_{sd} . If we devise a control law such that

$$s\dot{s} \leq -\eta|s|, \quad \eta > 0,\tag{9}$$

then we are assured to reach the sliding surface $s = 0$ within finite time given by $s(t = 0)/\eta$. Our job is now to construct, given the bounds on $f(\mathbf{x})$ and b , a control law such that system is driven to the sliding surface in the way prescribed by equation (9). We do this as follows.

Assume

$$\begin{aligned}F &\geq |f - \hat{f}| \quad \text{and} \\ b_{min} &\leq b \leq b_{max}\end{aligned}\tag{10}$$

Define

$$\hat{u} = -\hat{f} + (\ddot{y}_{sd}) - \lambda(\dot{y}_s - \dot{y}_{sd})\tag{11}$$

Where \dot{y}_{sd} is the desired lateral velocity at the sensor and \ddot{y}_{sd} is the desired lateral acceleration at the sensor location. Note that in our application these are identically zero. We have retained them for generality. The control input required to satisfy equation (9) is given by

$$\delta = (\hat{u} - k \operatorname{sgn}(s)) / \hat{b}\tag{12}$$

such that

$$\begin{aligned}k &\geq \beta(F + \eta) + (\beta - 1)|\hat{u}|, \\ \beta &= (b_{max}/b_{min})^{1/2}\end{aligned}\tag{13}$$

Note that uncertainties in V_x , K_{wy} , m , I_z , C_{α_r} , C_{α_f} etc are taken care of by appropriate choice of k . Sliding mode at $s = 0$ is guaranteed to take place. As a result, the lateral error at the sensor will go to zero. i.e.,

$$y_r + ds (\epsilon - \epsilon_d) \rightarrow 0.\tag{14}$$

But nothing can be said about the yaw error ($\epsilon - \epsilon_d$) or the lateral error y_r at the CG. Given $s = 0$ and small steering input δ , some “local” stability of the yaw and the lateral dynamics at CG can be shown. Note that the assumptions are weak and hold only for a small steering angle. If we assume that the steering angle remains small, then (refer figure 4),

$$\dot{y}_r \approx V_x(\epsilon - \epsilon_d). \quad (15)$$

This equation combined with equation (3) gives,

$$\dot{y}_s \approx V_x(\epsilon - \epsilon_d) + d_s(\dot{\epsilon} - \dot{\epsilon}_d). \quad (16)$$

Thus we see that,

$$\dot{y}_s \rightarrow 0 \quad \Rightarrow \quad (\dot{\epsilon} - \dot{\epsilon}_d) + V_x/d_s(\epsilon - \epsilon_d) \rightarrow 0$$

Hence, for local stability of yaw error in the above sense, V_x/d_s should be greater than zero. Similar conclusion can be derived for the lateral error dynamics about the CG.

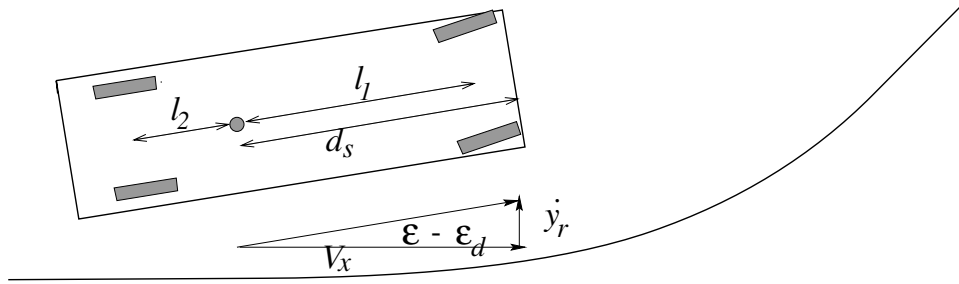


Figure 4: Scenario on a curve with small steering angle

Another problem appears as chatter in the input to the plant due to the presence of $k \operatorname{sgn}(s)$ in the controller output. One way to smooth the control is to use $\operatorname{sat}(s/\Phi)$ in place of $\operatorname{sgn}(s)$ in the control law. Φ is the boundary layer around the sliding surface where the control law is linear in s . Precisely, the control law is given by

$$\begin{aligned} \delta &= (\hat{u} - k \operatorname{sat}(s/\Phi)) / \hat{b} \\ \operatorname{sat}(s/\Phi) &= 1 \quad \Phi \leq s \\ \operatorname{sat}(s/\Phi) &= s \quad -\Phi \leq s < \Phi \\ \operatorname{sat}(s/\Phi) &= -1 \quad s < -\Phi \end{aligned} \quad (17)$$

where \hat{u}, k, s, \hat{b} are same as defined earlier. This method to eliminate chatter results in a compromise on tracking error. The reason is that the control law given by equation (17) satisfies a relaxed version of condition given by equation (9). The relaxed version is given by

$$\begin{aligned} s \geq \Phi &\Rightarrow \frac{d}{dt}[s - \Phi] \leq -\eta, \quad \eta > 0 \\ s \leq -\Phi &\Rightarrow \frac{d}{dt}[s + \Phi] \geq \eta \end{aligned} \quad (18)$$

A remedy is to redefine the sliding variable s as

$$s = \dot{e} + 2\lambda e + \lambda^2 \int_0^t e(\tau) d\tau \quad (19)$$

$$= (D + \lambda)^2 v(t) \quad (20)$$

where

$$v(t) = \int_0^t e(\tau) \quad (21)$$

$v(t)$ can be considered the output of the augmented plant (see figure 5). The relative degree of the augmented plant with respect to the new output and input δ has become three. Adopting the same SMC design methodology as earlier, we construct an input which will ensure the satisfaction of equation (18). Note that this condition ensures that the system reaches a band 2Φ thick around $s = 0$ in finite time and stays there. The control law is given by equation (17) with s given by equation (19) and \hat{u} given by

$$\hat{u} = -\hat{f} + (y_{s_d}^{\ddot{\cdot}}) - 2\lambda\dot{e} - \lambda^2 e \quad (22)$$

The gain k remains as defined in equation (10). Though the above control law does not imply the convergence of tracking error, e , the tracking error will be close to zero when the combined effect of the disturbances and uncertainties is nearly constant in the region $|s| < \Phi$. The overall system is depicted in figure 5. Note the presence of an integrator in the path from y_s to δ .

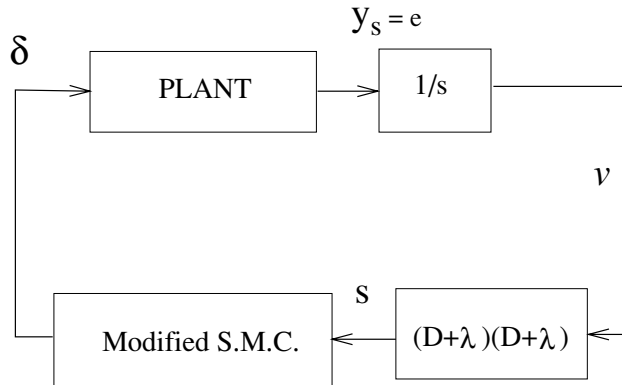


Figure 5: Block diagram of controller one

3.2 Sliding Mode Controller Design II

It is clear that the first controller does not guarantee, theoretically, that the yaw or the lateral dynamics of the CG will be stable in the large. In fact, after the addition of the boundary layer, tracking error convergence in y_s is also not assured. Another approach was applied to this problem by Ackermann et al. (1995) and the following approach is same

. The problem is tackled in two stages. First we find out a desired yaw rate such that it stabilizes the lateral dynamics at the sensor. Then we construct –using conventional SMC methodology– a controller which tracks the desired yaw rate.

Consider the following kinematical equation that we saw before.

$$\dot{y}_s = \dot{y}_r + d_s(\dot{e} - \dot{e}_d) \quad (23)$$

If we can provide yaw rate \dot{e} such that

$$\dot{e} = -\left(\frac{1}{d_s}\right)(\dot{y}_r + ky_s) + \dot{e}_d \quad k > 0 \quad (24)$$

then

$$\dot{y}_s + ky_s = 0 \quad (25)$$

is attained.

We are assured stable dynamics in y_s provided the actual yaw rate is kept close to the desired rate. We construct a SMC which will track the desired yaw rate described by equation (24).

The system in consideration is described by equation (1) which, restated is,

$$\begin{aligned} I_z \frac{d}{dt} \dot{e} &= 2l_2 C_{\alpha_r} (\dot{y} - \dot{e}l_2)/V_x - 2l_1 C_{\alpha_f} (\dot{y} + \dot{e}l_1)/V_x + 2l_1 C_{\alpha_f} \delta \\ \ddot{e} &= f_2(\mathbf{x}) + b_2 \delta \end{aligned} \quad (26)$$

Define the desired yaw rate given by equation (24) as \dot{e}_r . and the tracking error σ by

$$\sigma = \dot{e} - \dot{e}_r \quad (27)$$

sliding surface parameter s as

$$s \triangleq d_s \dot{\sigma} + \lambda d_s \sigma \quad \lambda > 0 \quad (28)$$

As in the previous section, we construct a control law such that

$$s\dot{s} \leq -\eta|s|, \quad \eta > 0 \quad (29)$$

Thus the sliding mode $s = 0$ is reached in finite time. Since $\lambda > 0$, the tracking error goes to zero asymptotically on the sliding surface. Then, noting equation (24), y_s goes to zero asymptotically. Because of the particular definition of the sliding surface, the equivalent control, given by $\dot{s} = 0$, contains the first time derivative of the steering input δ .

$$\begin{aligned} \dot{s} = 0 &\Rightarrow d_s(\ddot{\sigma} + \lambda\dot{\sigma}) = 0 \\ &\Rightarrow \dot{f}_2(\mathbf{x}) + b_2\dot{\delta} + \lambda f_2(\mathbf{x}) + \lambda b_2\delta - \ddot{e}_r - \lambda(\dot{e}_r) = 0 \end{aligned}$$

Which means that $\dot{\delta}$ has to be selected to satisfy the last equality. Thus we have to redefine the control input as $\dot{\delta}$. The dynamically extended system becomes

$$\begin{aligned}\frac{d}{dt}\dot{c} &= \ddot{c} \\ \frac{d}{dt}\ddot{c} &= \dot{f}_2(\mathbf{x}) + b_2\dot{\delta} \\ &\triangleq f^*(\mathbf{x}, \delta) + b_2\delta^* \\ \text{output} &= \dot{c}, \quad \text{input} = \delta^*\end{aligned}$$

Note that this extension is in the form of an integrator before the plant. We could, though, have used any first order filter instead.

Let the estimate of f^* be \hat{f}^* and the estimate of b_2 be \hat{b}_2 . Note that the estimates are in terms of the nominal parameter values and system state. Their bounds in terms of b_{2min} , b_{2max} and F are given by

$$b_{2min} \leq b_2 \leq b_{2max} \quad |\hat{f}^* - f^*| \leq F$$

we construct a control law δ^* given by

$$\delta^* = (\hat{u} - k \operatorname{sgn}(s))/\hat{b}_2 \quad (30)$$

where,

$$\hat{u} = -\hat{f}^* + \ddot{c}_r - \lambda(\ddot{c} - \ddot{c}_r).$$

and k must satisfy

$$k \geq \beta(F + \eta) + (\beta - 1)|\hat{u}|, \quad \beta = (b_{2max}/b_{2min})^{1/2}$$

This control law assures that the condition given by equation (29) hold. Let us look at the preceding material from a different view. It is of interest to note that the sliding variable s can be constructed from the sensor output, y_s , and its derivatives: i.e., noting equations (23), (24) and (28),

$$\begin{aligned}s &= (D + \lambda)d_s\sigma \\ &= (D + \lambda)(d_s\dot{c} - d_s\dot{c}_r) \\ &= (D + \lambda)(d_s\dot{c} + \dot{y}_r + ky_s - d_s\dot{c}_d) \\ &= (D + \lambda)(\dot{y}_s + ky_s) \\ &= (D + \lambda)(D + k)y_s\end{aligned}$$

Overall system is depicted in figure 6. We can see that this algorithm introduces an integrator in the feedback loop. The integrator is placed before the plant. It is of interest to compare this structure with the one in figure 5. The SMC scheme in figure 6 induces chattering of δ^* which is filtered by the integrator.

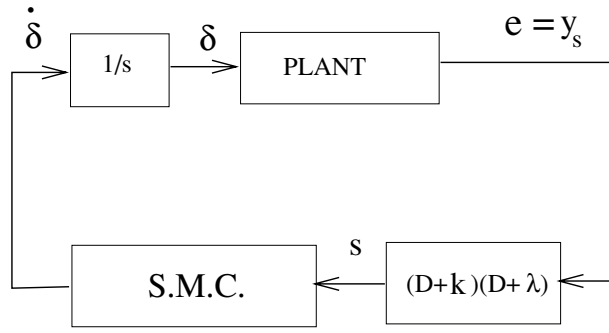


Figure 6: Block Diagram of the second controller seen as input filtering

4 Simulations

Simulations were performed for the following scenario. The bus has an initial condition such that the yaw error, lateral error and their time derivative are zero. d_s and V_x are $6m.$ and $25m/s.$ respectively. The road is straight for the first second i.e., $\dot{\epsilon}_d = 0,$ and then there is a right curve of radius $400m.$ Though the vehicle model used in the design of the controllers considered only the yaw and the lateral dynamics, the simulations are performed on the full twelve state model incorporating all six degrees of freedom of the vehicle. All controllers were realized in digitized form with a sampling period of $3ms.$

1. Controller 1 (design I). Simulations were performed for sliding surface pole, $\lambda = 5.6$ for the controller without integrator term and with $\lambda = 2.6$ for the controller with the integrator term. We present simulations done with the first controller without integral term so that we have a reference to judge the relative performance with respect to this “normal” controller. The boundary layer thickness was kept at a uniform value of 0.04 in both cases. The parameter variation was introduced in the inertia of the bus. In the following figures (7 - 15) “Heavy plant” means that the inertia was 1.3 times the nominal inertia. “Light plant” means that the inertia was about $1/1.3$ of the nominal value. Along with the lateral error $y_s,$ its components, y_r and $(\epsilon - \epsilon_d)d_s$ (shown as $er^*ds,$ where er stands for $(\epsilon - \epsilon_d)$) are also plotted.

In controller 1, without the addition of the integral term in the definition of the sliding surface, a steady state tracking error in y_s appears due to the introduction of the boundary layer (see figures 7 - 9). This is rectified by the addition of the integrator on the output side of the plant. Theoretical claims cannot be made about asymptotic tracking in general. Nevertheless, we see that in the present case the addition of the integrator works (see figures 10 - 12). That the steering rate is below the specified limit of $0.5rad/s$ cannot be verified. The tracking performance is satisfactory. Since all states are assumed available, this is unrealistically good.

2. Controller 2 (design II). Simulations were performed for the sliding surface parameter $\lambda = 2.6.$ The value of the parameter k in equation 24 was taken as $2.5.$ figures 13 - 15 show that for all the parameter ranges the steering angle is smooth for the controller

2. The steering rate sent out by the controller is, however, switching. We can see that this chatter is filtered quite effectively by the integrator (see figure 6). The steering angle rate is well within the 0.5 rad/s limit. The tracking performance, judged by y_s , is satisfactory.

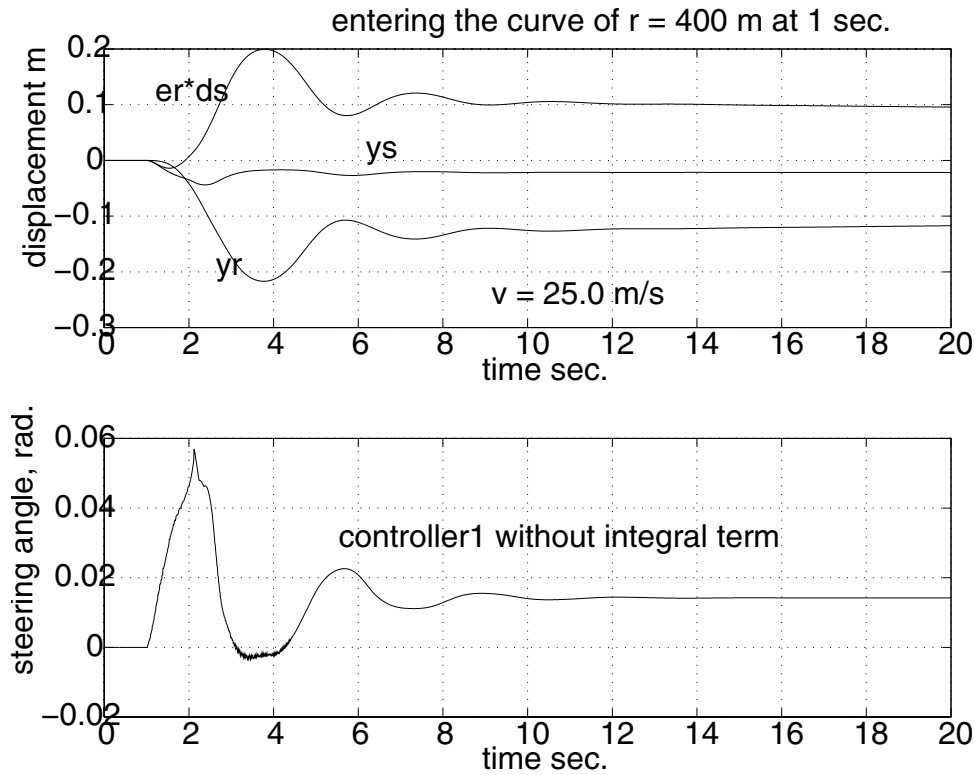


Figure 7: Simulation for first controller and light plant

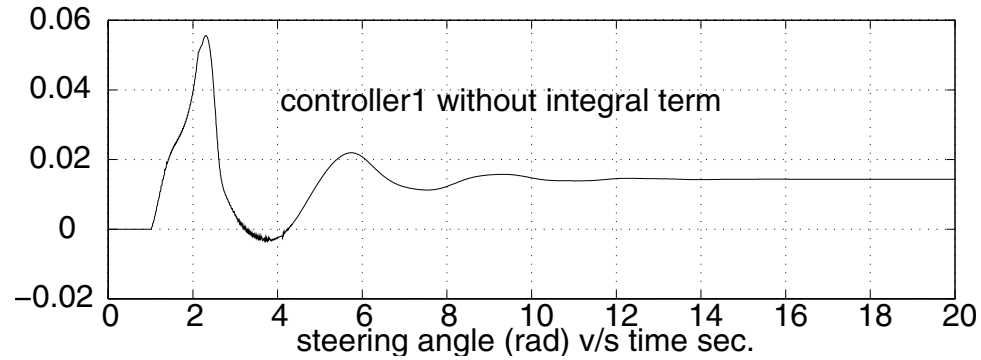
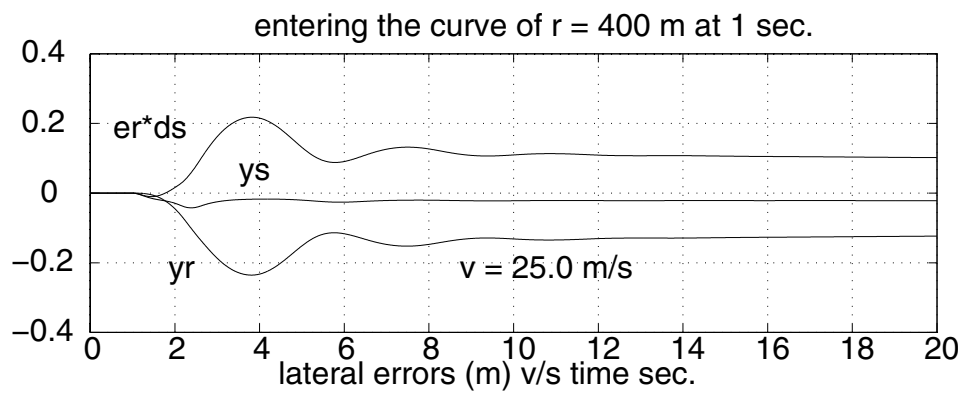


Figure 8: Simulation for first controller and nominal plant

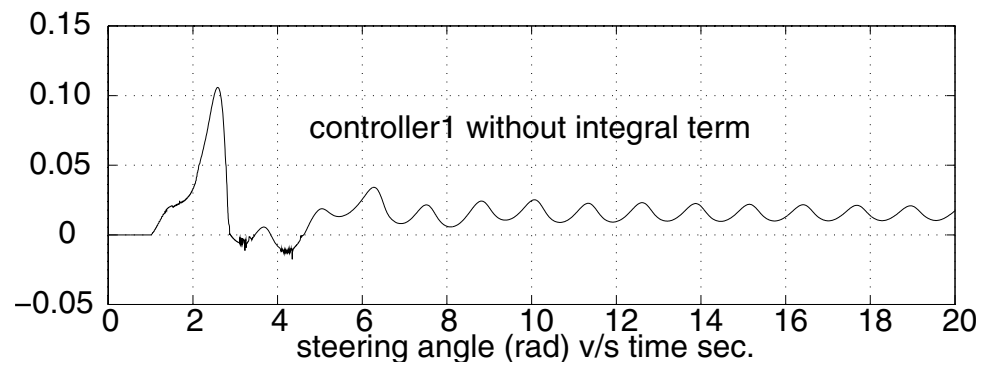
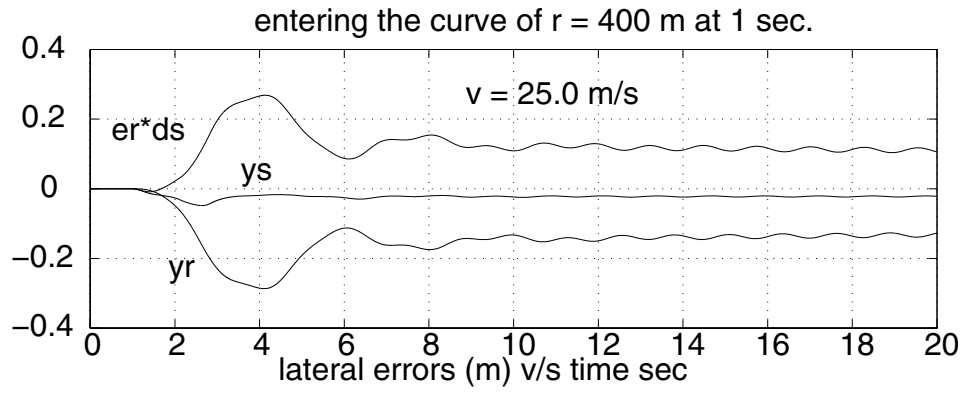


Figure 9: Simulation for first controller and heavy plant

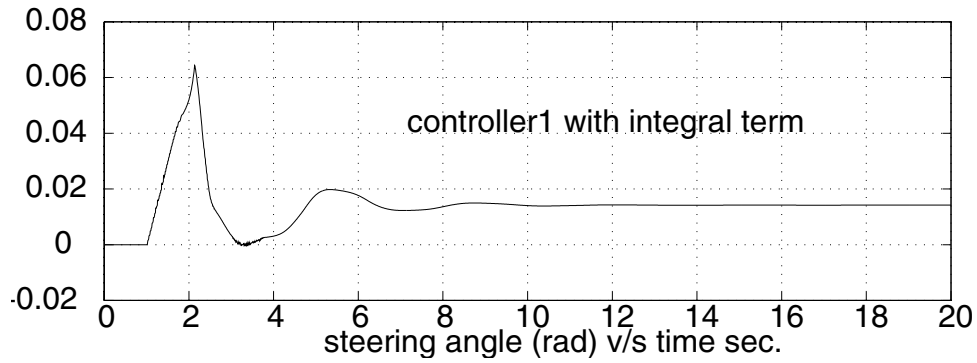
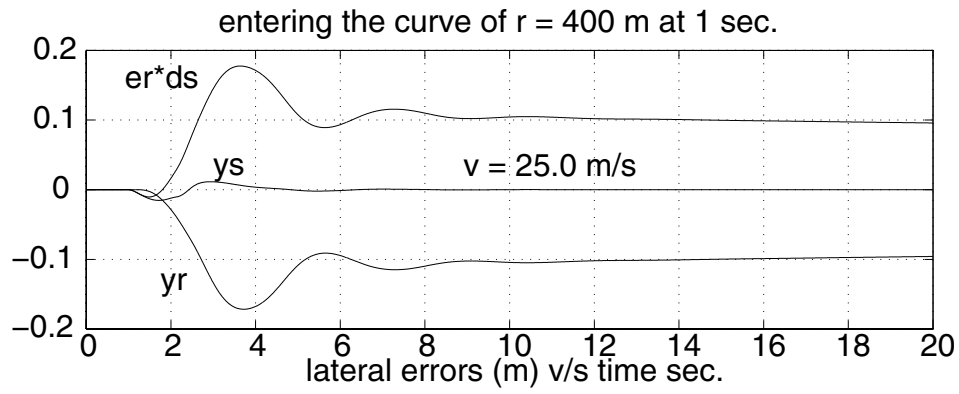


Figure 10: Simulation for first controller and light plant (Integrator added)

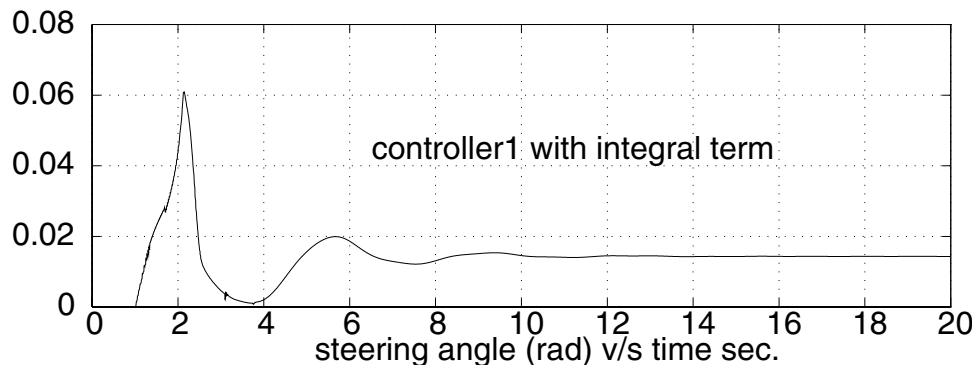
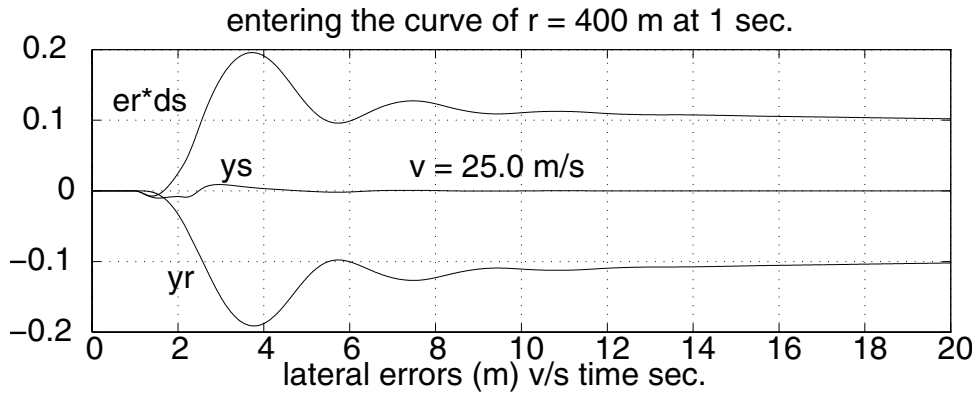


Figure 11: Simulation for first controller and nominal plant (Integrator added)

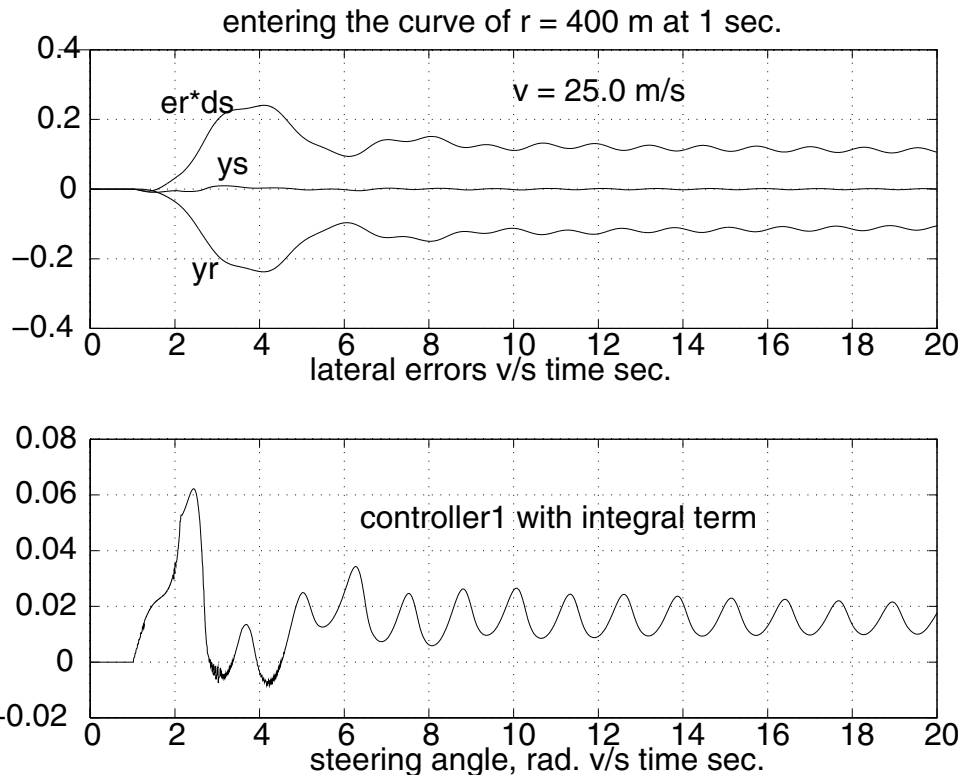


Figure 12: Simulation for first controller and heavy plant (Integrator added)

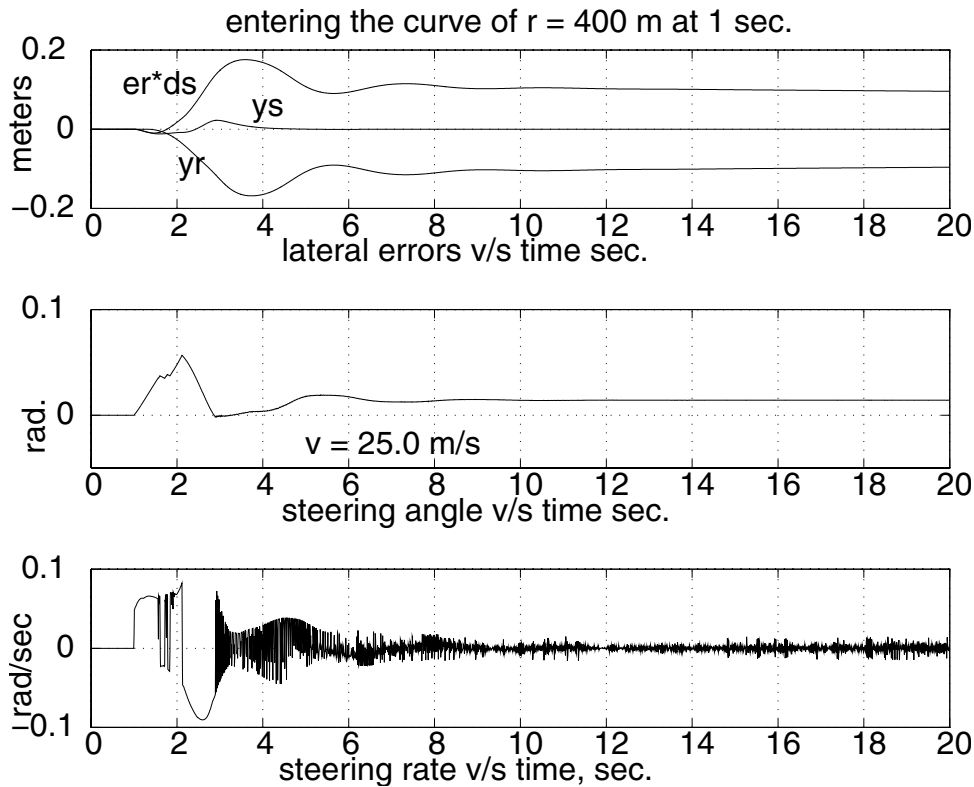


Figure 13: Simulation for second controller and light plant

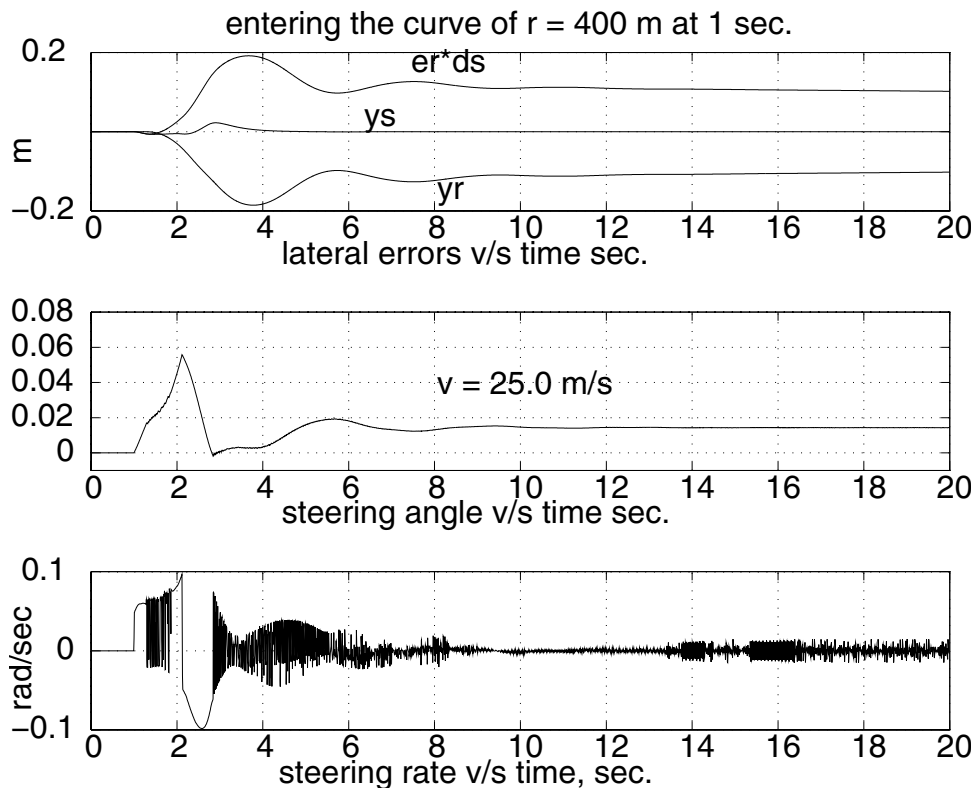


Figure 14: Simulation for second controller and nominal plant

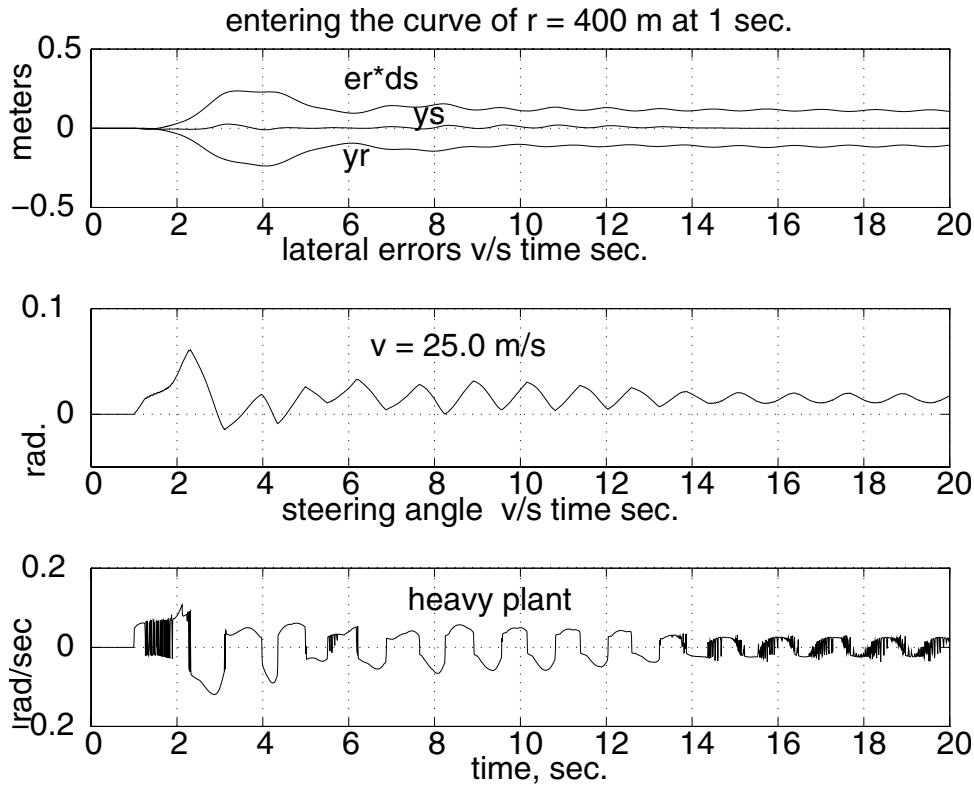


Figure 15: Simulation for second controller and heavy plant

5 Conclusion

Two SMC based controllers were applied to the problem of lateral control of commuter buses. The reduction of the chatter, which appears in the control action due to the presence of the *sign* function in SMC design, was one of the objectives. Boundary layer was added to smooth the control in the first approach. This prompted addition of an integral term in the definition of the sliding surface, which showed up as an integrator at the output end of the plant. In simulations, the tracking error, after addition of the integral term in the definition of the sliding surface, converged to zero. However, we lose the robust asymptotic property of the Sliding Mode Control design methodology. In general lateral error convergence to zero cannot be guaranteed. Also, since we are introducing the integrator on the output side, integrator windup may be a problem. In the second controller, an integrator naturally appeared in the feed back loop but at the input of the plant. This eliminated the chatter in the input to the plant. The ideal sliding mode was maintained. Hence asymptotic error convergence to zero is guaranteed. From an implementation point of view, the simulations with the second controller gives a more realistic idea of the tracking performance, as a steering actuator can be naturally inserted at the place of the integrator in figure 6.

The performance of the controllers with regard to the ride quality could not be addressed. But there is a possibility, using the second approach, filtering off those frequencies in the plant input which may potentially excite roll dynamics. This is the topic of future research. Also, given the present scenario for passenger vehicles, assumption that all the states are available through measurement is not reasonable. So issues regarding use of observer and proper sensors need to be addressed.

References

- [1] Peng, H. and M. Tomizuka. 1993. "Preview Control for Vehicle Lateral Guidance in Highway Automation," *ASME Journal of Dynamic Systems, Measurement and Control*, Vol. 115, No. 4, pp. 678-686.
- [2] Pham, H., K. Hedrick and M. Tomizuka. 1994. "Combined Lateral and Longitudinal Control of Vehicles," *Proceedings of the American Control Conference*, Baltimore, Maryland, pp. 1205-1206.
- [3] Ackermann, J., J. Guldner, W. Sienel, R. Steinhauser. 1995. "Linear and Nonlinear Controller Design for Robust Automatic Steering," *IEEE Trans. on Control Systems Technology*, Vol 3, pp. 132-143.
- [4] Bareket Z., Fancher P. 1989. "Representation of Truck Tire Properties in Braking and Handling Studies, Influence of Pavement and Tire Conditions on the Friction Characteristics," UMTRI-8933
- [5] Peng, H. 1992. "Vehicle Lateral Control for Highway Automation," PhD dissertation, University of California, Berkeley.
- [6] Patwardhan, S., 1994, "Fault Detection and Tolerant Control for Lateral Guidance of Vehicles in Automated Highways," PhD dissertation, University of California, Berkeley.
- [7] Slotine, J. and W. Li. 1991. *Applied Nonlinear Control*, Prentice Hall.
- [8] Utkin, V. 1978. *Sliding Modes and Their Application in Variable Structure Systems*, MIR Publisher, Moscow.
- [9] Matsumoto, N. and M. Tomizuka. 1992. "Vehicle Lateral Velocity and Yaw Rate Control with Two Independent Inputs," *ASME Journal of Dynamic Systems, Measurement and Control*, Vol 114, pp. 606-612.